UC Irvine
UC Irvine Previously Published Works

Title
Enhanced antigen presentation and immunostimulation of dendritic cells using acid-degradable cationic nanoparticles

Permalink
https://escholarship.org/uc/item/24x0f11g

Journal
Journal of Controlled Release, 105(3)

ISSN
0168-3659

Authors
Kwon, Young Jik
Standley, Stephany M
Goh, Sarah L
et al.

Publication Date
2005-07-01

DOI
10.1016/j.jconrel.2005.02.027

Peer reviewed

eScholarship.org Powered by the California Digital Library
University of California

Since January 2020 Elsevier has created a COVID-19 resource centre with free information in English and Mandarin on the novel coronavirus COVID-19. The COVID-19 resource centre is hosted on Elsevier Connect, the company's public news and information website.

Elsevier hereby grants permission to make all its COVID-19-related research that is available on the COVID-19 resource centre - including this research content - immediately available in PubMed Central and other publicly funded repositories, such as the WHO COVID database with rights for unrestricted research re-use and analyses in any form or by any means with acknowledgement of the original source. These permissions are granted for free by Elsevier for as long as the COVID-19 resource centre remains active.

Available online at www.sciencedirect.com

SCIENCE DIRECT®

Journal of Controlled Release 105 (2005) 199–212

journal of controlled release

www.elsevier.com/locate/jconrel

Enhanced antigen presentation and immunostimulation of dendritic cells using acid-degradable cationic nanoparticles

Young Jik Kwon, Stephany M. Standley, Sarah L. Goh, Jean M.J. Fréchet*,[1]

Center for New Directions in Organic Synthesis, University of California, Berkeley, CA 94720, United States
Department of Chemistry, University of California, 718 Latimer Hall, Berkeley CA 94720-1460, United States
Materials Sciences Division, Lawrence Berkeley National Laboratory, Berkeley, California 94720, United States

Received 29 December 2004; accepted 24 February 2005
Available online 1 June 2005

Abstract

Acid-degradable cationic nanoparticles encapsulating a model antigen (i.e., ovalbumin) were prepared by inverse microemulsion polymerization with acid-cleavable acetal cross-linkers. Incubation of these degradable nanoparticles with dendritic cells derived from bone marrow (BMDCs) resulted in the enhanced presentation of ovalbumin-derived peptides, as quantified by B3Z cells, a $CD8^+$ T cell hybridoma. The cationic nature of the particles contributed to the increased surface endocytosis (or phagocytosis) observed with BMDCs, which is the first barrier to overcome for successful antigen delivery. The acid sensitivity of the particles served to direct more ovalbumin antigens to be processed into the appropriately trimmed peptide fragments and presented via the major histocompatibility complex (MHC) class I pathway following hydrolysis within the acidic lysosomes. It was also shown that adjuvant molecules such as unmethylated CpG oligonucleotides (CpG ODN) and anti-interleukin-10 oligonucleotides (AS10 ODN) could be co-delivered with the protein antigen for maximized cellular immune response.
© 2005 Elsevier B.V. All rights reserved.

Keywords: Degradable nanoparticle; Antigen presentation; Dendritic cells; Adjuvant oligonucleotides; Cancer vaccine

1. Introduction

Since being introduced roughly two centuries ago for smallpox, vaccines have significantly contributed to human health as one of the most effective tools in preventing and treating fatal diseases. Traditionally, either whole inactivated or live attenuated microorganisms are injected, however, this method sometimes leads to side effects that range from mild to unacceptable. Recently, purified or recombinated macromolecules of pathogens, such as surface proteins or polysaccharides, have been used increasingly in clinical trials to minimize the possible side effects. As additional knowledge of the workings of the immune system on a molecular level is acquired,

* Corresponding author. Department of Chemistry, University of California, 718 Latimer Hall, Berkeley CA 94720-1460, United States. Tel.: +1 510 643 3077; fax: +1 510 643 3079.
E-mail address: frechet@cchem.berkeley.edu (J.M.J. Fréchet).
[1] The Center for New Directions in Organic Synthesis is supported by Bristol-Myers Squibb as a Sponsoring Member and Novartis Pharma as Supporting Member.

0168-3659/$ - see front matter © 2005 Elsevier B.V. All rights reserved.
doi:10.1016/j.jconrel.2005.02.027

more efforts can be directed towards the development of highly efficient but safe vaccines for diseases such as AIDS and cancers that have previously eluded treatment via vaccination [1–3]. Cancer immunotherapy has been identified as one of the most plausible alternatives to conventional chemotherapy, radiotherapy, and surgery as it possesses many unique advantages. These include highly specific delivery to targeted cells, memory to pre-immuned diseases, and simple administrations (e.g., injection, inhalation of aerosol vaccine, and skin patch) [4]. As more detailed information of the mechanism of the disease becomes available, the delivery of therapeutic molecules has become one of the most important targets for the development of a successful vaccination strategy.

Activation of the immune system by a vaccine requires (i) the delivery of a sufficient amount of antigen to antigen presenting cells (APCs, macrophages and dendritic cells), (ii) the controlled presentation of antigen molecules to target immune cells ($CD4^+$ and/or $CD8^+$ T cells), (iii) the proliferation of effector cells such as cytotoxic T lymphocytes (CTLs) and plasma B cells, and (iv) the maintenance of an activated immune system for the desired period of time [5]. However, no universal vaccine system displaying all of these requirements has been developed thus far. To deliver antigens to phagocytic APCs, various delivery systems such as liposomes, microparticles, and nanotubes have been studied [6–8]. Using these delivery vehicles, the antigens mixed with adjuvant molecules, such as bacterial lipopolysaccharide (LPS), have demonstrated prolonged immune responses and increased local inflammation [9].

Once internalized, antigens are processed by either an endogenous or an exogenous pathway. Endogenous antigen-derived peptides are presented on major histocompatibility complex (MHC) class I molecules, which activate a cytotoxic T lymphocyte (CTL)-mediated immune response, or cellular immunity, after binding to T cell receptors. In contrast, an antibody-mediated response, also referred to as humoral immunity, is activated through exogenous antigen-derived peptide/MHC II complexes on APCs. Therefore, it is presumed that a desirable immune response can be achieved by controlling the antigen presentation pathway and cellular immune response has been reported to be more effective in removing infected cells and cancers than humoral immunity [10]. In previous studies, it has been shown that an increased MHC I antigen presentation can be achieved by priming APCs with antigen-encapsulating acid-degradable nanoparticles, which degrade at acidic pH following phagocytosis to release the antigens into the cytoplasm [11–13].

In this study, a model antigen, ovalbumin, was encapsulated in cationic acid-degradable nanoparticles. Incubation with the most potent professional APCs, dendritic cells (DCs), resulted in an increased endocytosis of the nanoparticles and presentation of ovalbumin on MHC I molecules by DCs. It was also shown that maximized immune responses might be achieved simply by coating adjuvant oligonucleotides on the cationic surface of the nanoparticles.

2. Materials and methods

2.1. Preparation of acid-degradable cationic nanoparticles

The degradable nanoparticles were prepared by an inverse microemulsion polymerization method as follows. Non-ionic surfactants (3 : 1 Span 80 : Tween 80, Aldrich, St. Louis, MO), were dissolved in hexane at the concentration of 10% (w : w), and air was removed by sparging with dry nitrogen overnight. An aqueous solution of monomers was prepared by dissolving acrylamide (Biorad, Hercules, CA), 2-acryloxyethyltrimethylammonium chloride (AETMAC, Aldrich), 5 mg ammonium persulfate (APS, Biorad), and acid-labile benzyl acetal cross-linker [13] in 200 μL of phosphate buffered saline (PBS, pH 8.0) containing 10 mg/mL of ovalbumin (Sigma, St. Louis, MO). The aqueous solution of monomers was combined with 20 mL of the organic surfactant solution. After vigorously shaking the mixture for 1 min, polymerization was initiated by the addition of 20 μL of *N*,*N*,*N*́,*N*́-tetramethylethylenediamine (TEMED, Sigma). The mixture was stirred for 10 min before adding an excess of acetone (1.5–2 times the volume of the organic surfactant solution) to settle the clumped nanoparticles, followed by an additional 10 min of gentle stirring. After standing 1 h, the precipitated pellet was washed once with acetone and dried under vacuum overnight. By changing the ratio of AETMAC to acrylamide,

various cationic nanoparticles were prepared at a fixed crosslinking ratio of 5%. For comparison, non-degradable polyacrylamide nanoparticles were made using acrylamide and *N*,*N*′-methylenebisacrylamide (Biorad).

2.2. Nanoparticle characterization

The size and surface charge of the nanoparticles were measured using a dynamic light scattering (DLS) particle sizer and zeta potential analyzer (Zetasizer Nano ZS, Malvern Instruments, Malvern, UK). The nanoparticles were suspended at 1 mg/mL in pH 7.4 PBS (Gibco BRL, Bethesda, MD) for the size measurement and in pH 7.5 buffer made of 5 mM HEPES and 1 mM NaCl for zeta-potential analysis. For transmission electron microscopy (TEM), the nanoparticle suspension in PBS was spotted onto a formvar/carbon grid (Ted Pella, Redding, CA). After 5 min the grid was washed with distilled water twice and then dried at room temperature for 2 h. To minimize hydrolysis of the particles, the samples were examined immediately after drying with a Philips Tecnai 12 transmission electron microscope with 100 kV. The diameters of 100 randomly chosen nanoparticles were estimated from the TEM image by using NIH Image (version 4.02, NIH, Bethesda, MD). The amount of protein encapsulated was determined using ovalbumin that had been conjugated with pH-insensitive cascade blue dye (Molecular Probe, Eugene, OR). The labeled protein was prepared according to the protocol provided by the manufacturer. The particles were hydrolyzed by incubating with 300 mM acetic acid buffer pH 5.0 for 3 h at room temperature. Ovalbumin concentrations were quantified by measuring the cascade blue fluorescence, obtained by exciting the solutions at 355 nm and detecting the emitted 405 nm wavelength using a fluorescence plate reader.

2.3. Bone marrow-derived dendritic cells (BMDCs)

Dendritic cells were obtained using a slightly modified literature procedure [14]. Briefly, femurs and tibia of 2–4 month old female C57BL/6 mice (Jackson Laboratory, Bar Harbor, ME) were extracted after euthanasia, and the bone marrow was flushed out using a 26 gauge needle with 5 mL of RPMI1640 medium supplemented with 10% (v/v) fetal bovine serum (FBS) (Hyclone, Logan, UT), 100 U/mL penicillin, 100 μg/mL streptomycin, 2 mM L-glutamine, 1 mM sodium pyruvate, and 55 μM 2-mercaptoethanol (all from Gibco). After the red blood cells were removed by treating with RBC lysis buffer (Gentra Systems, Minneapolis, MN), the remaining cells were cultured with the medium given earlier and further supplemented with 5% (v/v) of granulocyte-macrophage colony stimulating factor (GM-CSF)-containing supernatant, a generous donation from Dr. Edward James (UC Berkeley) [15]. After 7 days of cultivation in a 6-well plate, the suspended cells were inoculated onto a 96-well plate in the density of 5×10^4 cells/well.

2.4. Antigen presentation assay

The amount of presented ovalbumin-derived peptide $OVA_{258–265}$ (or SIINFEKL) with MHC class I molecule (K^b) was measured by an in vitro cellular assay and an immunoassay. BMDCs were incubated with varying amounts of ovalbumin-loaded nanoparticles for 6 h and then washed extensively with pH 7.4 PBS. B3Z $CD8^+$ T cell hybridomas (1×10^5 cells/well) were co-incubated overnight with BMDCs. This hybridoma expresses lacZ upon binding of the T cell receptor (TCR) to SIINFEKL/K^b [16]. The medium was replaced with 100 μL of CPRG buffer containing 91 mg of chlorophenol red β-D-galactopyranoside (CPRG, Roche, Indianapolis, IN), 1.25 mg of NP40 (EMD Sciences, La Jolla, CA), 9 mL of 1 M $MgCl_2$ (Aldrich), and 1 L of PBS. The amount of the lacZ enzyme was quantified by the hydrolysis of CPRG, which produces chlorophenol red absorbing at 595 nm. The quantity of SIINFEKL/K^b was calculated by comparison with the UV absorption values obtained from free SIINFEKL peptide incubated with DCs as a reference. To minimize the pH drop that might result from lactic acid accumulation, particles were added in fresh medium and incubated with DCs for 1 and 6 h for the particle uptake and antigen presentation experiments, respectively. No change in color of the medium was observed during these experiments suggesting that no significant pH change had taken place since a slight pH drop would have turned the medium yellow (since phenol red works at very narrow range of pH 6.4–8.0).

To visualize the SIINFEKL/K^b complex density on the BMDC surface, 1×10^6 cells were cultured on 2.2 cm round collagen I-coated coverslips (BD Biosciences, Bedford, MA) in one well of a 6-well plate and incubated with 0.5 mg of the nanoparticles in 2 mL of medium for 6 h. After washing with PBS twice, the cells were fixed with 1% paraformaldehyde buffer, followed by washing with PBS+5% FBS. Cells were further incubated for 1 h at 4 °C with a 25-D1.16 monoclonal antibody (mAb) supernatant produced from B cell hybridoma, which was gifted from Dr. Ronald Germain (NIAID, NIH, Bethesda, MD) [17]. After washing with PBS+5% FBS, 1 μg of R-phycoerythrin(PE)-conjugated goat anti-mouse polyclonal antibody (Pharmingen, San Diego, CA) was added in 1 mL of PBS+5% FBS, and the cells were incubated for an additional hour at 4 °C. After washing twice, the coverslip was placed on a glass slide and examined using a LS450 laser-scanning confocal microscope (Carl Zeiss, Thornwood, NY).

2.5. Endocytosis and cytotoxicity assay

Ovalbumin was conjugated with fluorescein-like pH-insensitive Alexa Fluor 488 succinimidyl ester (Molecular Probes). BMDCs were incubated with 0.5 mg of labeled ovalbumin-loaded nanoparticles per well of a 6-well plate for 1 h, washed, trypsinized, and analyzed using a Beckman-Coulter EPICS XL-MCL flow cytometer. The kinetics of endocytosis by BMDCs were determined by examining the mean channel value, which is the average fluorescence intensity above threshold level (i.e., fluorescence by untreated cells as a reference). To test for cytotoxicity, 5×10^4 BMDCs per well of a 96-well plate were incubated with various amounts of acid-degradable cationic nanoparticles for 6 h. After extensively washing three times with the medium, the cells were cultured for additional 48 h. The medium was aspirated, and 10 μL of a stock solution containing 10 mg/mL of 3-(4,5-dimethylthiazol-2-yl)-2,5-diphenyltetrazolium bromide (MTT, Sigma) in PBS was added along with 90 μL of medium, followed by further incubation for 3 h at 37 °C. The reduced MTT-formazan product generated by live cells was dissolved in 200 μL of dimethylsulfoxide, and 20 μL of glycine buffer (0.1 M glycine, 0.1 M NaCl, pH 10.5) was added. Relative viability of the cells incubated with nanoparticles to untreated cells was determined by measuring the MTT-formazan absorbance at 561 nm.

2.6. Nucleic acid-coated nanoparticles

Immunostimulatory unmethylated CpG oligonucleotide (CpG ODN) 5′ TCCATGACGTTCCTGACGTT 3′ [18] and anti-IL-10 oligonucleotide (AS10 ODN) 5′ CATTTCCGATAAGGCTTGG 3′ [19] were synthesized using an Expedite 8909 DNA synthesizer (Applied Biosystems, Foster City, CA). A solution of 10 μg of CpG ODN in 0.5 mL of PBS was mixed with 0.5 mL of 10% cationic ovalbumin-encapsulating nanoparticles (0.5 mg/mL) and incubated on ice for 10 min with periodic mixing. The nanoparticles were washed by resuspending in 1 mL of the medium after centrifugation at 14,000 rpm for 30 s twice. A solution of 100 μL of the resuspended nanoparticles in the medium was added per well of a 96-well plate, where 5×10^4 BMDCs had been inoculated the day prior. AS10 ODN (20 μM) was adsorbed in the same manner as for CpG ODN. After 24 h of cultivation, the amount of interleukin-12 (IL-12) and IL-10 produced was quantified using an enzyme-linked immunosorbent assay (ELISA) kit (Pierce, Rockford, IL).

2.7. Data analysis

Data were obtained in triplicate unless otherwise mentioned and are presented as mean ± standard deviation, and further statistically analyzed by the student *t*-test on the significance level of $p < 0.05$.

3. Results

3.1. Synthesis of cationic nanoparticles degradable at lysosomal pH

The acid-degradable cationic nanoparticles were synthesized by inverse microemulsion polymerization of acrylamide **1**, quaternary amine monomer AETMAC **2**, and acid-labile acetal cross-linker **3** using a modification of the method reported previously [11,12] (Fig. 1). The microemulsion was achieved by vigorous shaking instead of sonication, as the latter may potentially damage the encapsulated molecules. Since it was found that particles pelleted by centrifu-

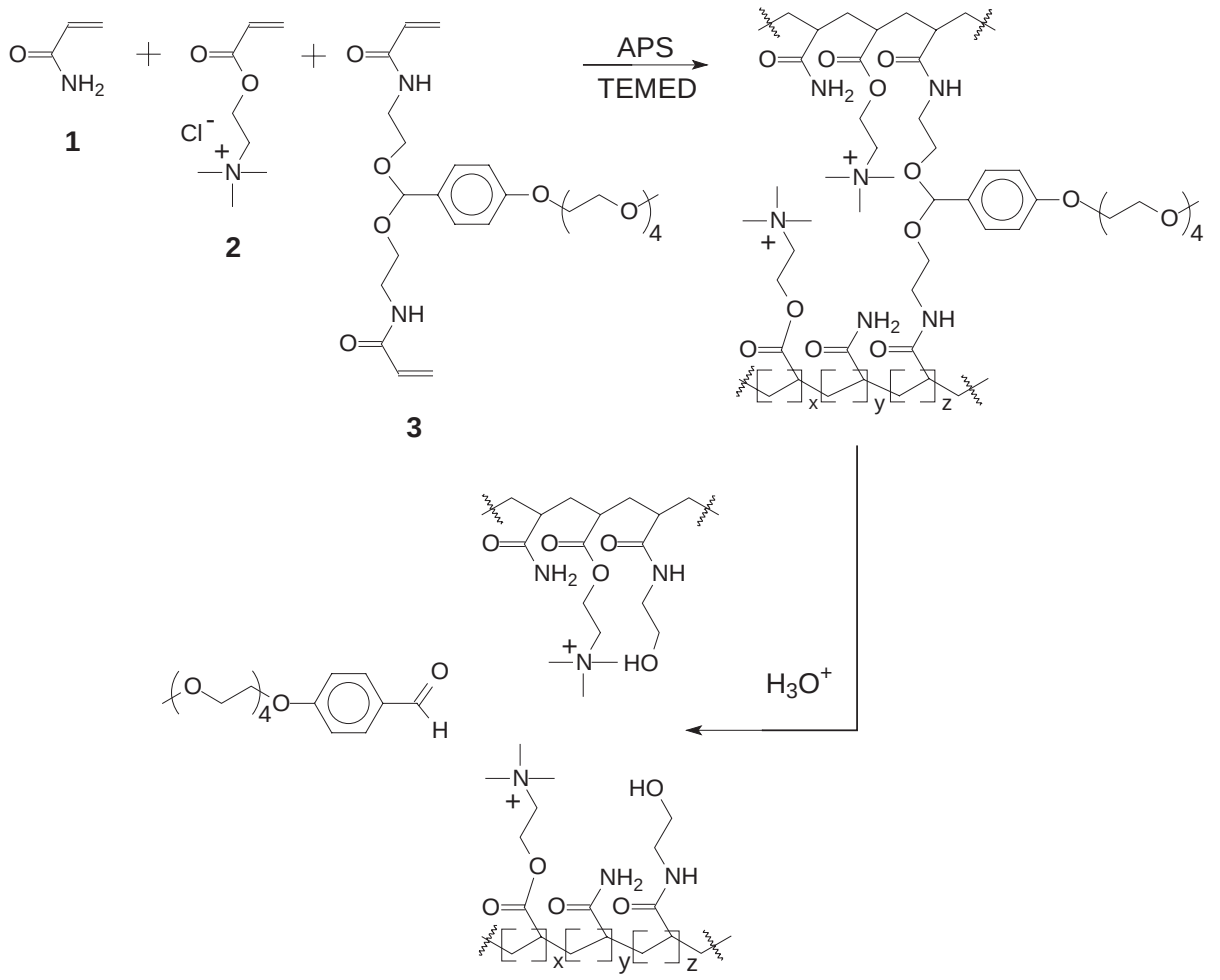

Fig. 1. Preparation of cationic acid-degradable nanoparticle by polymerization of acrylamide and a cationic monomer with cleavable acetal cross-linker. Under the acidic conditions found in the lysosome, the cross-linkers are cleaved thus releasing the encapsulated antigens.

gation were not always readily resuspended in aqueous solutions, the nanoparticles were harvested by precipitation using gravity only. After treating with acetone, the surfactants present on the surface of the particles were washed away and the cationic surfaces were exposed to non-polar hexane solvent. Following settling of visible clumps of aggregated particles a second acetone wash was performed to remove the proteins on the surface of the particles. The degree of cationic surface charge was easily manipulated by varying the ratio of acrylamide to AETMAC monomers (Table 1). Although increased antigen presentation has been achieved using acid-degradable particles, and facilitated internalization of cationic molecules has also been reported. This study is, to our knowledge, the first to explore the simultaneous realization of both of these major goals.

Table 1
Formulation of various acid-degradable nanoparticles and ovalbumin encapsulation efficiency

Cationic ratio [x/(x+y)](%)[a]	Encapsulation efficiency (μg ovalbumin/mg nanoparticles)
0	32.34 ± 0.35
5	43.88 ± 1.91
10	40.60 ± 3.81
20	29.32 ± 0.10

[a] Fixed crosslinking ratio [z/(x+y+z)]=5%.

3.2. Characterization of acid-degradable cationic nanoparticles

The size of various cationic and neutral nanoparticles in PBS was measured using dynamic light scattering. Regardless of the cationic monomer ratio, the DLS results showed that the size of particles ranged between 180–230 nm in diameter (Fig. 2a), which bridges the size regimes for pinocytosis and phagocytosis [20]. Transmission electron microscopy (TEM) also confirmed the size distribution, giving an average diameter of 217 ± 49 nm (Fig. 3). Therefore, the particles are expected to be taken up exclusively by phagocytic cells (e.g., macrophages and dendritic cells) in a size-dependent passive targeting. Since a reduced uptake of latex particles larger than 280 nm by DCs was reported previously [21], the smaller particles prepared here can be efficiently taken up by DCs. Although particles with 10% and 20% cationic monomer displayed a slightly smaller diameter, the content of cationic monomer did not significantly affect particle size distributions (Fig. 2a). A similar size distribution was observed with non-degradable nanoparticles prepared in similar fashion. As expected, zeta potential, or relative positive charge density, increased as the ratio of cationic monomer to acrylamide was increased (Fig. 2b).

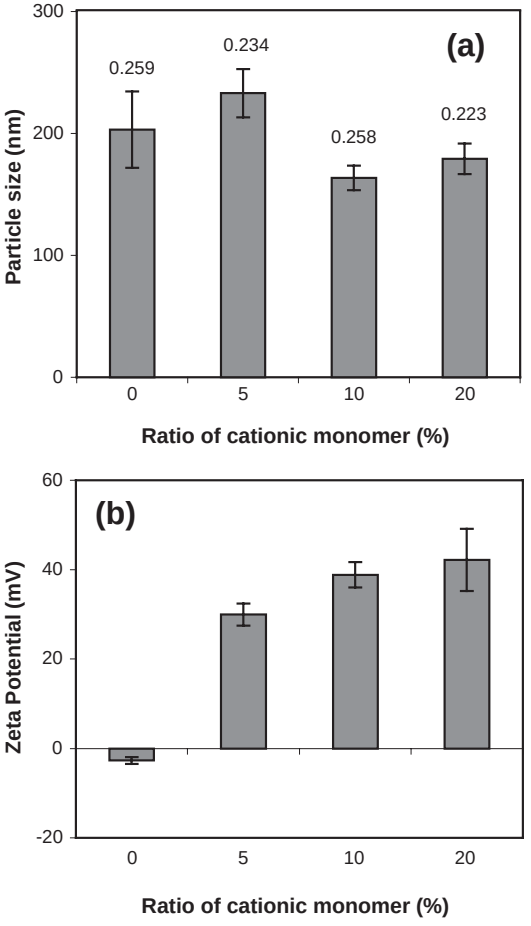

Fig. 2. Analysis of cationic acid-degradable nanoparticles: (a) size (Z-average) measured by dynamic light scattering particle sizer with the polydispersity index (PDI) given above each bar; (b) surface charge by zeta-potential analyzer.

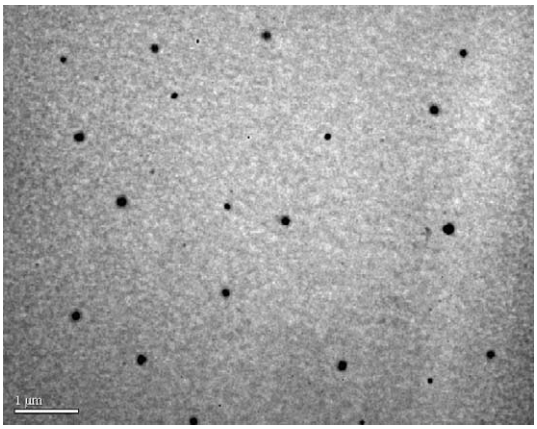

Fig. 3. Transmission electron micrograph of the nanoparticles made with 10% cationic monomer (% with respect to acrylamide). Nanoparticles with different formulations also showed the similar size distribution. The scale bar represents 1 μm.

Antigen payload was determined by hydrolysis of the acid-degradable nanoparticles containing encapsulated cascade blue labeled-ovalbumin. The highest ovalbumin payloads were achieved with particles prepared with 5% and 10% cationic monomers, resulting in encapsulation efficiencies of 43.88 and 40.60 μg/mg, respectively (Table 1). Neutral and 20% cationic acid-degradable nanoparticles exhibited 25% lower encapsulation efficiencies compared to the 5% and 10% cationic nanoparticles. The amount of encapsulated proteins in non-degradable particles cannot be determined using the method used with degradable particles (due to the lack of degradability of the former). Spectroscopic data obtained with the non-degradable and degradable particle solutions after incubation in NaOH solution were very close. This

suggests that the amounts of encapsulated protein are comparable in the non-degradable and the degradable particles.

3.3. Enhanced antigen presentation on MHC class I by DCs using acid-degradable nanoparticles

For effective CTL activation, antigens must be presented by MHC I molecules carrying the antigen-derived peptides that have been processed in the cytoplasm. To determine if the acid-degradability of the particles increases the release of encapsulated protein into the cytosol and, hence, increases antigen presentation by MHC I, acid-degradable and non-degradable particles with various cationic ratios were prepared and incubated with BMDCs. The relative amounts of ovalbumin-derived peptide SIINFEKL with K^b (MHC I) presented by BMDCs were quantified by cultivation with the B3Z hybrima T cell line. Overall, more SIINFEKL peptides were presented with MHC I after delivery in acid-degradable nanoparticles than in non-degradable ones (Fig. 4). Therefore, acid-degradability aids in the release of ovalbumin into the cytoplasm, where proteins are cleaved by proteasomes, and integrated with MHC I in the endoplasmic reticulum (ER). This is because it is thought that the particles are taken up by APCs through phagocytosis then transferred to the acidic lysosome. The acid sensitivity of the cross-linker holding the particles together not only helps to release protein from the particle, but also their delivery to the cytoplasm [12]. Ovalbumin encapsulated in non-degradable particles is expected to be released more slowly and would therefore be more susceptible to degradation by the proteases present in the lysosome.

More peptides were presented when delivered in neutral acid-degradable nanoparticles at high concentration (i.e., 250–500 μg/well), while 10% and 20% cationic nanoparticles were more effective in antigen delivery and presentation at lower concentrations (25–50 μg/well). The 10% cationic nanoparticles showed the highest efficiency of SIINFEKL presentation on K^b at the concentration of 50 μg/well (Fig. 4a). The lowest antigen presentation—even lower than with neutral particles—was observed with 5% cationic nanoparticles, at the concentrations of 5–50 μg/well. No detectable antigen presentation was seen using 20% cationic nanoparticles at the concentration of 250 μg/well, whereas the neutral particles showed maximum presentation at this same concentration (Fig. 4a). With non-degradable nanoparticles, antigen presentation levels were higher for cationic particles than for neutral particles at concentrations of 5–50 μg/well (Fig. 4b). The maximum antigen presentation for non-degradable particles was achieved by using 10% cationic particles at the concentration of 50 μg/well, as was the case with the acid-degradable particles. Thus it appears that 10% cationic acid-degradable nanoparticles used at the concentration of 50 μg/well consti-

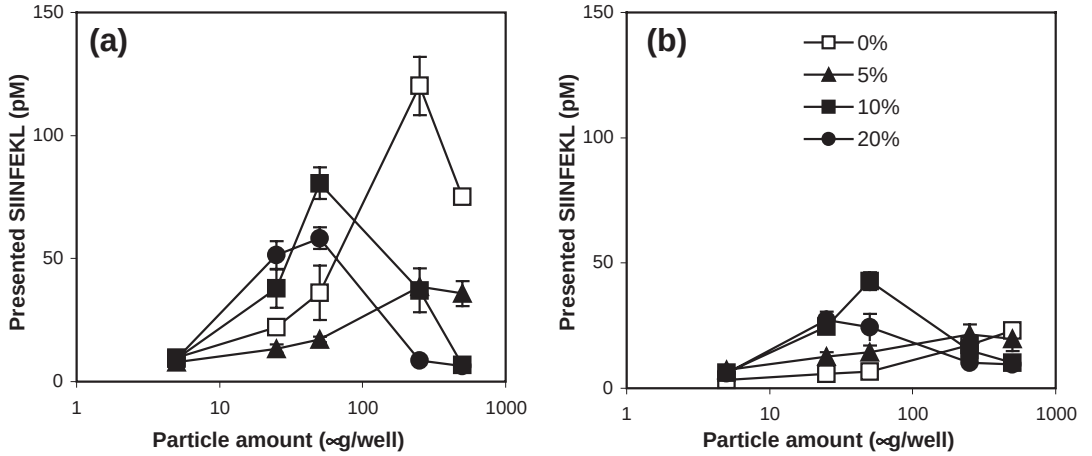

Fig. 4. Antigen presentation by BMDCs incubated with ovalbumin-encapsulating (a) acid-degradable and (b) non-degradable nanoparticles with various cationic ratios.

tute the most potent antigen delivery system to BMDCs.

Staining BMDCs with SIINFEKL/K^b-specific mAbs clearly showed an increase in antigen presentation using the acid-degradable nanoparticles (Fig. 5). Without particles, the cells themselves exhibit a minimal amount of autofluorescence (Fig. 5a). Encapsulation of ovalbumin in acid-degradable particles increases the signal observed by the fluorescent antibody, indicative of a higher concentration of SIINFEKL peptides being presented at the cell surface. The highest fluorescence signal was observed when the BMDCs were exposed to 10% acid-degradable cationic nanoparticles rather than neutral particles (Fig. 5c). These results correlates with the antigen presentation data given in Fig. 4, in which the 10% cationic particles also exhibit a higher presentation than the neutral particles at the concentration of 50 μg/well.

3.4. Increased endocytosis of cationic nanoparticles

To assess the usefulness of the cationic carriers for enhanced cellular uptake, cationic and neutral acid-degradable nanoparticles encapsulating ovalbumin labeled with pH-insensitive fluorescent dye Alexa Fluor 488® were incubated with BMDCs for 1 h, followed by flow cytometry analysis. Cells incubated with cationic nanoparticles showed a higher fluorescence intensity, indicative of more internalized particles, than the cells incubated with neutral nanoparticles (Fig. 6). Some of the cells (~20%) incubated with neutral nanoparticles showed higher fluorescence than the others, possibly an artifact of the polydispersity of the particles. The cells that take up larger particles, most likely containing more of the fluorescent ovalbumin, showed higher fluorescence intensity (see the arrow on Fig. 6a). The particle uptake kinetics showed that increased endocytosis of cationic nanoparticles occurred throughout the incubation period of 1 h (Fig. 6c). The fluorescence reached a plateau after 1 h because all of the protein had been processed. Typically, an antigen is degraded and processed inside a cell within a timeframe of 0.5–3 h. The saturation of uptake corresponding to the plateau in fluorescence might be mainly due to the balance between the endocytosis and antigen processing. It should be noted that the fluorescence measurements gave similar results when performed after 1 h with gentle mixing every 15 min (data not shown).

3.5. Cytotoxicity of cationic nanoparticles

At high concentration of acid-degradable nanoparticles, decreased antigen presentation was observed, as shown in Fig. 4. This result could be due to the cationic nature of the particles. Cationic delivery vehicles such as polyethyleneimine (PEI) and poly-L-lysine (PLL) have been shown to inhibit cellular viability and proliferation, even though they are efficiently taken up by cells [22]. To determine the toxicity of our delivery system, acid-degradable cationic nanoparticles were incubated with BMDCs for 6 h, and the relative viability was quantified using the conventional MTT assay. Results showed that the cytotoxicity of the nanoparticles increases with con-

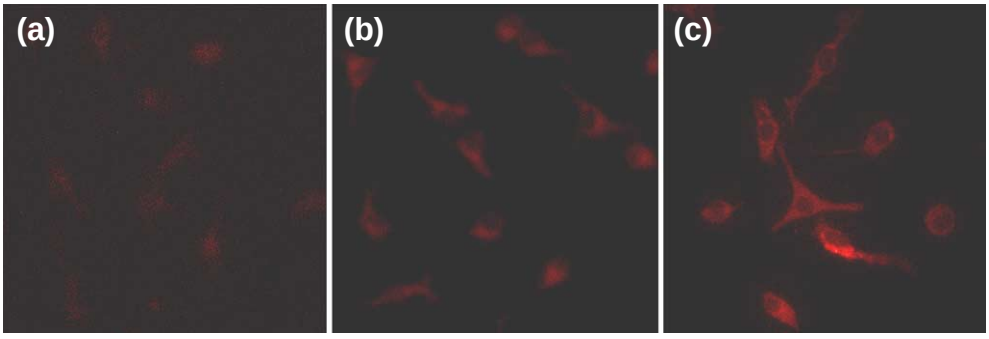

Fig. 5. Laser-scanning confocal micrographs of BMDCs stained with SIINFEKL/K^b specific monoclonal 25.D1-16 antibodies after incubated (a) without nanoparticles, (b) with ovalbumin-encapsulating acid-degradable neutral nanoparticles, and (c) acid-degradable 10% cationic nanoparticles for 6 h (magnification of ×800).

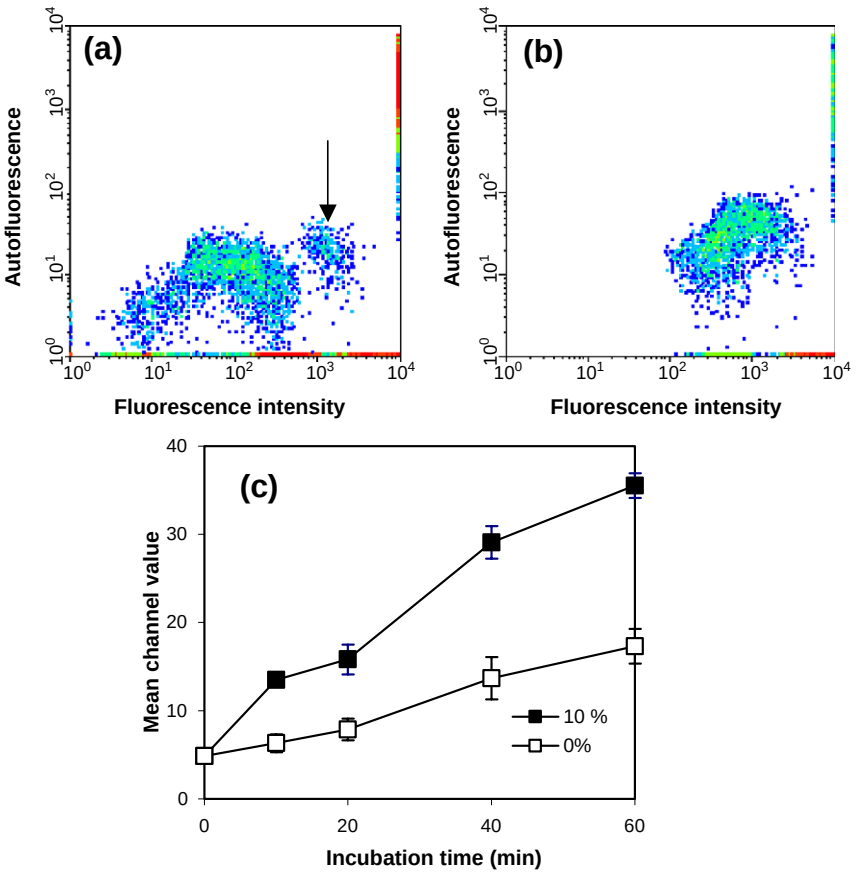

Fig. 6. Endocytosis of (a) acid-degradable neutral nanoparticles and (b) acid-degradable 10% cationic nanoparticles by BMDCs after 1 h incubation, and endocytosis kinetics of (c) acid-degradable 10% cationic nanoparticles and neutral nanoparticles by BMDCs. Arrow indicates the cells with higher fluorescence intensity possibly due to uptake of larger particles.

centration regardless of the cationic ratio (Fig. 7). Even 20% decreased viability was observed with neutral nanoparticles at the highest concentration of 500 μg/well, where antigen presentation was dramatically decreased (Fig. 4a). Possible explanations for the observed cytotoxicity of neutral acid-degradable nanoparticles include: (i) the existence of a threshold amount of particles that can be processed without retarding cellular proliferation; (ii) the intrinsic toxicity of polyacrylamide in the cell; and (iii) the cytotoxicity of the benzaldehyde released after hydrolysis. The 10% and 20% cationic nanoparticles, especially the 20% sample, showed significant cytotoxicity at the concentrations of 250 and 500 μg/well (Fig. 7) with decreased antigen presentation (Fig. 4a). However, at the concentration of 50 μg/well, comparable cytotoxicity of neutral and 10% cationic nanoparticles

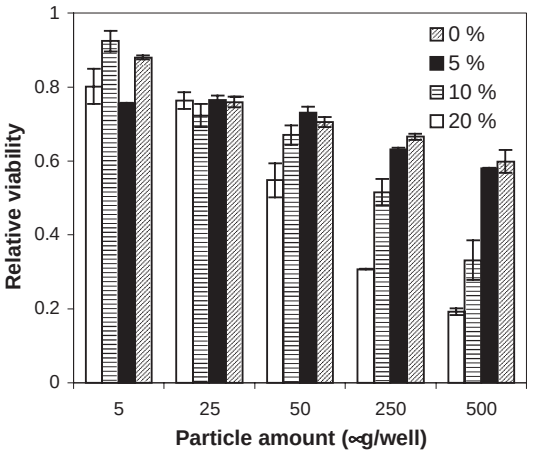

Fig. 7. Cytotoxicity of acid-degradable nanoparticles with various cationic ratios at different concentrations.

was observed, while 20% cationic nanoparticles showed significantly lower proliferation. Given these toxicity and antigen presentation studies, the most efficient cationic delivery system at a reasonably acceptable concentration appears to be that with 10% cationic monomer at a concentration of 50 μg/well equivalent to 0.25 mg/mL. These particles displayed the highest antigen presentation (Fig. 4a), with high proliferation (Fig. 7), and a more efficient uptake due to the positive surface charge (Figs. 5c and 6).

3.6. Cytosolic release and DC maturation by degradable nanoparticles

In order to visualize the fate of the proteins taken up in the lysosomal compartment and their eventual release into the cytoplasm, DCs were incubated with fluorescently labeled nondegradable and acid-degradable 10% cationic nanoparticles. As can be seen in Fig. 8, the intracellular fate of the two different types of nanoparticles was quite different. Ovalbumin fluorescently labeled with Alexa Fluor 488®, then encapsulated and delivered via nondegradable particles was observed to remain confined within a restricted intracellular area (Fig. 8a, dark arrow). In contrast fluorescence was observed throughout the cells incubated with labeled acid-degradable particles (Fig. 8b). It was also noticed that nondegradable particles tended to form aggregates, which were not observed with degradable particles (Fig. 8a, white arrow). This is because the degradable particles made with the tetraglyme-conjugated cross-linkers possess enhanced dispersibility as reported previously [13].

The morphologies of BMDCs incubated with 10% cationic nondegradable or degradable particles indicated a very unexpected effect of the particle degradability on DC maturation (Fig. 8). Immature DCs are specialized in antigen capture whereas mature DCs present degraded peptides with upregulated MHC II, and costimulatory and adhesion molecules. One of the typical features of mature DCs is the unique morphology with long and thin dendrites, which are thought to be advantageous for maximizing antigen presentation and T cell junctions. Very interestingly, BMDCs incubated with 10% cationic degradable nanoparticles displayed a highly dendritic surface (Fig. 8b), while similar dendritic cells incubated with 10% cationic nondegradable particles showed an immature stellate shape (Fig. 8a). This observation suggests that degradable particles enhance antigen presentation not only by releasing encapsulated proteins into the cytoplasm but also by triggering DC maturation. Although lysosomal disruption by acid-degradable particles seems to cause BMDC maturation, a mechanism for this event is not clear at this time. Obviously, DC maturation would constitute another advantage for the use of acid-degradable vaccine carrier as a result of such enhanced immune activation.

3.7. Delivery of CpG and anti-IL-10 oligonucleotides for maximized immune response

DCs bridge the innate nonspecific immune system and the highly specific adaptive immunity through several mechanisms, one of which is mediated by Toll like receptors (TLR) that recognize unique mo-

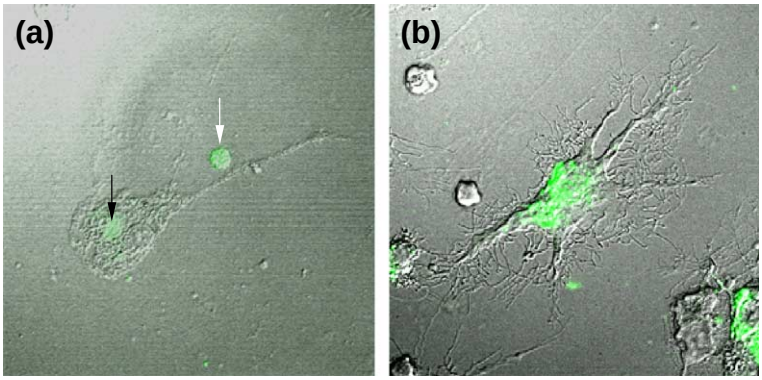

Fig. 8. Combined differential interface-contrast (DIC) and laser-scanning confocal micrographs of BMDCs incubated with 10% cationic nondegradable (a) and acid-degradable nanoparticles (b) for 6 h. Intracellular particle location was confirmed by varying focus planes.

lecular patterns of pathogens and activate cellular pathways required to functionalize the immune responses. Immunostimulatory unmethylated CpG ODN was coated on the acid-degradable 10% cationic nanoparticles and incubated with BMDCs for 24 h. Activation of the DCs was then quantified by IL-12 secretion, which polarizes $CD4^+$ T helper cell type 1 (T_H1) differentiation rather than T_H2 and eventually assists in CTL activation. Fig. 9a clearly illustrates that BMDCs produced at least 10 times more IL-12 after incubation with CpG ODN-coated acid-degradable nanoparticles than controls of cells alone, BMDCs incubated with free CpG ODN, or the nanoparticles without CpG ODN. Similarly, AS10 ODN was adsorbed onto the cationic acid-degradable nanoparticles. The secretion of IL-10, an antagonist cytokine to IL-12, by BMDCs was inhibited by delivery of AS10 ODN. A 60% decrease in IL-10 secretion was observed when the oligonucleotide was combined with cationic nanoparticles (Fig. 9b). Therefore, the formulation of acid-degradable cationic nanoparticles can be tuned to produce the maximum CTL-mediated immune response by stimulating IL-12 secretion and inhibiting IL-10 expression by DCs.

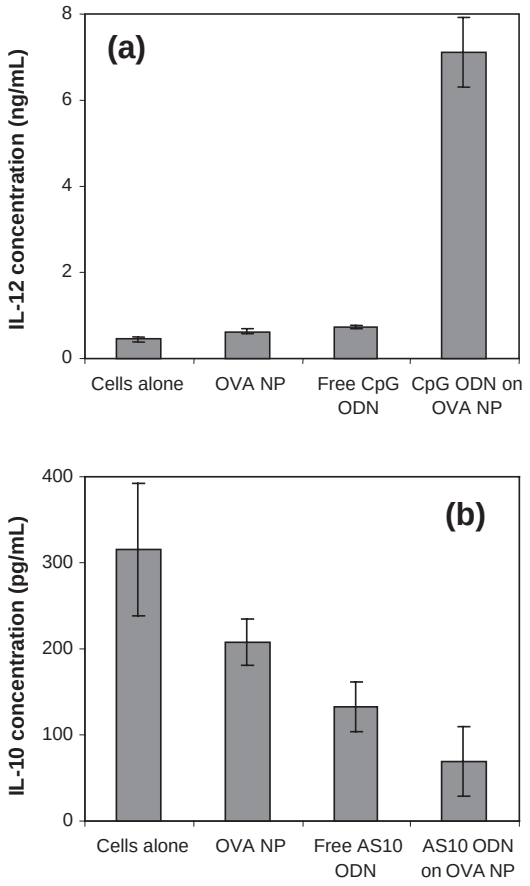

Fig. 9. (a) Secretion of IL-12 by BMDCs incubated with acid-degradable 10% cationic nanoparticles coated with unmethylated CpG oligonucleotide (CpG ODN) and (b) IL-10 secretion by BMDCs incubated with 10% cationic nanoparticles coated with anti-IL-10 oligonucleotides (AS10 ODN) for 24 h.

4. Discussion

Numerous interesting studies have been carried out since vaccines have been reconsidered as a preventive and therapeutic tool against cancer, one of the major causes of death in western societies. However, it was discovered that simply injecting cancer antigens was not sufficient to activate an anti-cancer immune response, as not only cancer cells but also normal cells express the same antigen (i.e., cancer-associated antigen) [5]. Frequently, cancer cells downregulate MHC molecules so that expression of cancer antigens is insufficient [23]. Once established, cancer cells also secrete cytokines and form new rigid tumor tissue as a defense against immune attack [24]. Therefore, developing an efficient cancer vaccine is urgently needed. As more knowledge and understanding of cancer becomes available, and as more unique cancer antigens are identified, the design of an effective antigen delivery vehicle becomes more critical. The ideal carrier should possess the properties of specific targeting, efficient antigen delivery, activation of proper immune responses, facile and inexpensive preparation, and simple administration and storage.

In this study, acid-degradable cationic nanoparticles have been used to deliver a model antigen, ovalbumin, to BMDCs. More evidence has been accumulated indicating that DCs play pivotal roles in orchestrating immune responses: activation and tolerance [25,26]. DCs reside in antigen-encountering areas, such as under the skin and the mucosal layer. After antigen uptake and maturation, DCs migrate to lymphoid organs such as the spleen and lymph nodes and activate naïve T and B cells by very efficiently presenting antigen-derived peptides with costimula-

tory molecules, resulting in the secretion of cytokines at high concentrations upon activation [27,28]. DCs are also more susceptible than other cells to viral infections like human inmmunodeficiency virus type 1 (HIV-1) and severe acute respiratory syndrome (SARS) coronavirus so that viral antigens are presented efficiently [29,30]. It has also been shown that DCs link innate immunity with adaptive immunity. Therefore, it is a general consensus that the targeting and priming of DCs is a critical target for the development of a successful vaccine strategy.

It was demonstrated that acid-degradable nanoparticles are significantly more effective in antigen presentation by MHC I than non-degradable nanoparticles (Fig. 4). A possible explanation for this finding is that more proteins are released into cytoplasmic space with the acid-degradable particles than is the case with the non-degradable ones. It was previously hypothesized that release of the small molecule aldehyde after hydrolysis might destabilize the lysosomal membrane due to increased osmotic pressure [12], followed by cytosolic release of the antigen. In addition, the swelling effect of the hydrogel nanoparticles resulting from the cross-linker cleavage may also contribute to the more facile release as swelling could lead to a leaky lysosomal membrane structure. However, more studies must be undertaken to clarify the cellular behavior of acid-degradable particles since there is still a dearth of supporting evidence for endosomal (or lysosomal) escape of extracellular molecules. For example, it was believed that a polycationic polymer (e.g., PEI) aided in endosomal escape by the proton sponge effect. However, this theory was recently criticized by some studies with various protonated groups indicating no difference in endosomal escape [31,32]. As shown in Fig. 8, the degradability of the particles favors distribution of the antigenic payload throughout the cytoplasmic space, thereby contributing to more efficient presentation of antigen-derived peptides through DC maturation. Another possible explanation of the enhanced antigen presentation is the protection of proteins from lysosomal degradation in the encapsulated microenvironment of the nanoparticles, slowing or even negating the effect of proteases and minimizing exposure to the degrading conditions of the lysosome as a result of fast release into the cytoplasm. Therefore, more proteins would be successfully processed in the cytoplasm and presented on MHC I molecules.

Cationic molecules are well known to be easily internalized by most cells, including phagocytes such as macrophages and DCs, due to the attractive interactions with negatively charged proteoglycans on the cell surface [33,34]. It has also been shown that relatively large cationic particles, even as large as a few microns in diameter, could be taken up by DCs very efficiently [35,36]. Our cationic nanoparticles are designed to be efficiently endocytosed to help increase delivery efficiency since the more antigen proteins are delivered, the more antigen-derived peptides will be presented, therefore increasing the probability of encounter with T cells.

A drawback with cationic molecules is their cytotoxicity and therefore the amount administered must be kept to a minimum, which may result in low efficiency. However, it was demonstrated in this study that the cationic nanoparticles could deliver ovalbumin more efficiently than neutral ones while the toxicity of the two types of nanoparticles remained comparable at low concentration (i.e., 25–50 μg in 200 μL).

In addition to the advantage of using a cationic carrier for increased endocytosis, the cationic surface of the particle can adsorb anionic molecules such as DNA and negatively biased proteins. In previous studies, polylactide-*co*-glycolic acid (PLGA) particles coated with cationic surfactant effectively adsorbed plasmid DNA and oligonucleotides [37–39]. It was also shown that GM-CSF, which has isoelectric points of 4.6–4.9, was adsorbed and delivered on cationic particles [40]. The nanoparticles used in this study have also demonstrated the ability to adsorb negatively charged DNA and the cationic surface ratio was easier to modulate with these nanoparticles than was the case with previously reported systems.

Due to the progress in immunology, it has been revealed that an immune response is the result of the cell–cell interactions in very complicated networks under strict control. This response is mediated by surface molecules (e.g., receptors) and/or secreted macromolecules (e.g., cytokines). Once an unmethylated CpG DNA binds to TLR9 located under the cell surface and migrates to an endosomal or lysosomal compartment, APCs are activated to secrete cytokines (e.g., IL-12) and to upregulate costimulatory surface

molecules (e.g., B7) [41,42]. A recent study reported that TLR also regulates the maturation of the phagosome [43]. Therefore, delivering CpG DNA helps CTL activation by upregulating costimulatory molecules on the DC surface and encouraging the secretion of T_H1-polarizing IL-12. This directed immunostimulatory response can be maximized by suppressing antagonistic IL-10 secretion, for example, which can be accomplished by delivering antisense oligonucleotides, as shown in this study (Fig. 9). Interestingly, some studies have indicated that the cross-presentation—presentation of extracellular antigen by MHC I—of CpG DNA-conjugated proteins was induced by DCs [44,45]. This means that CpG DNA helps not only to stimulate innate immunity but also amplifies CTL-mediated immunity (or cellular immunity) rather than humoral immunity by cytokine release and cross-presentation. Therefore, it is expected that the cationic nature of the acid-degradable nanoparticles used in this study can be very useful as cancer vaccine carriers capable of adjusting immune responses.

5. Conclusions

Cationic acid-degradable nanoparticles can be used as carriers of a model antigen-ovalbumin—for protein-based vaccine development. The enhanced MHC I-mediated antigen presentation that is observed appears to be related to the acid-degradability of the particles. Cationic particles are endocytosed more efficiently than neutral ones, although the amount and cationic density of the particles requires optimization due to the innate cytotoxicity of cationic species. Finally, maximized cellular immunity can be achieved by delivering antigens with adjuvant nucleotides adsorbed onto the cationic surface of the acid-degradable particles.

Acknowledgements

Financial support of portions of this work by the National Institute of Health (Grant RO1EB002047) and, in part, by U.S. Department of Energy (Grant DE-ACO3-76SF00098) for the development of stimuli responsive nanoparticles is acknowledged with thanks.

References

[1] N.L. Letvin, B.D. Walker, Immunopathogenesis and immunotherapy in AIDS virus infections, Nat. Med. 9 (7) (2003) 861–866.
[2] E. Gilboa, The promise of cancer vaccines, Nat. Rev., Cancer 4 (5) (2004) 401–411.
[3] O.J. Finn, Cancer vaccines: between the idea and the reality, Nat. Rev., Immunol. 3 (8) (2003) 630–641.
[4] M.M. Levine, M.B. Sztein, Vaccine development strategies for improving immunization: the role of modern immunology, Nat. Immunol. 5 (5) (2004) 460–464.
[5] D.M. Pardoll, Spinning molecular immunology into successful immunotherapy, Nat. Rev., Immunol. 2 (4) (2002) 227–238.
[6] J. Kunisawa, S. Nakagawa, T. Mayumi, Pharmacotherapy by intracellular delivery of drugs using fusogenic liposomes: application to vaccine development, Adv. Drug Deliv. Rev. 52 (3) (2001) 177–186.
[7] A.G. Coombes, E.C. Lavelle, P.G. Jenkins, S.S. Davis, Single dose, polymeric, microparticle-based vaccines: the influence of formulation conditions on the magnitude and duration of the immune response to a protein antigen, Vaccine 14 (15) (1996) 1429–1438.
[8] D. Pantarotto, C.D. Partidos, R. Graff, J. Hoebeke, J.-P. Briand, M. Prato, A. Bianco, Synthesis, structural characterization, and immunological properties of carbon nanotubes functionalized with peptides, J. Am. Chem. Soc. 125 (20) (2003) 6160–6164.
[9] V.E. Schijns, Immunological concepts of vaccine adjuvant activity, Curr. Opin. Immunol. 12 (4) (2000) 456–463.
[10] A.F. Ochsenbein, Principles of tumor immunosurveillance and implications for immunotherapy, Cancer Gene Ther. 9 (12) (2002) 1043–1055.
[11] N. Murthy, Y.X. Thng, S. Schuck, M.C. Xu, J.M.J. Frechet, A novel strategy for encapsulation and release of proteins: hydrogels and microgels with acid-labile acetal cross-linkers, J. Am. Chem. Soc. 124 (42) (2002) 12398–12399.
[12] N. Murthy, M. Xu, S. Schuck, J. Kunisawa, N. Shastri, J.M.J. Frechet, A macromolecular delivery vehicle for protein-based vaccines: acid-degradable protein-loaded microgels, Proc. Natl. Acad. Sci. U. S. A. 100 (9) (2003) 4995–5000.
[13] S.M. Standley, Y.J. Kwon, N. Murthy, J. Kunisawa, N. Shastri, J.M.J. Fréchet, Acid-degradable particles for protein-based vaccines: enhanced survival rate for tumor challenged mice using ovalbumin model, Bioconjug. Chem. 15 (6) (2004) 1281–1288.
[14] K. Inaba, M. Inaba, N. Romani, H. Aya, M. Deguchi, S. Ikehara, S. Muramatsu, R.M. Steinman, Generation of large numbers of dendritic cells from mouse bone marrow cultures supplemented with granulocyte/macrophage colony-stimulating factor, J. Exp. Med. 176 (6) (1992) 1693–1702.
[15] E. James, D. Scott, J.-G. Chai, M. Millrain, P. Chandler, E. Simpson, HY peptides modulate transplantation responses to skin allografts, Int. Immunol. 14 (11) (2002) 1333–1342.
[16] N. Shastri, F. Gonzalez, Endogenous generation and presentation of the ovalbumin peptide/K^b complex to T cells, J. Immunol. 150 (7) (1993) 2724–2736.

[17] A. Porgador, J.W. Yewdell, Y. Deng, J.R. Bennink, R.N. Germain, Localization, quantitation, and in situ detection of specific peptide-MHC class I complexes using a monoclonal antibody, Immunity 6 (6) (1997) 715–726.
[18] M. Merad, T. Sugie, E.G. Engleman, L. Fong, In vivo manipulation of dendritic cells to induce therapeutic immunity, Blood 99 (5) (2002) 1676–1682.
[19] B.-G. Kim, H.-G. Joo, I.-S. Chung, H.Y. Chung, H.-J. Woo, Y.-S. Yun, Inhibition of interleukin-10 (IL-10) production from MOPC 315 tumor cells by IL-10 antisense oligodeoxynucleotides enhances cell-mediated immune responses, Cancer Immunol. Immunother. 49 (8) (2000) 433–440.
[20] B. Alberts, A. Johnson, J. Lewis, M. Raff, K. Roberts, P. Walter, Molecular Biology of the Cell, 4th ed., Garland Science, New York, NY, 2002.
[21] J.C. Reece, N.J. Vardaxis, J.A. Marshall, S.M. Crowe, P.U. Cameron, Uptake of HIV and latex particles by fresh and cultured dendritic cells and monocytes, Immunol. Cell Biol. 79 (2001) 255–263.
[22] D. Fischer, T. Bieber, H.-P. Elsasser, T. Kissel, A novel nonviral vector for DNA delivery based in low molecular weight, branched polyethyleneimine: effect of molecular weight on transfection efficiency and cytotoxicity, Pharm. Res. 16 (8) (1999) 1273–1279.
[23] B. Seliger, C. Harders, U. Wollscheid, M.S. Staege, A.B. Reske-Kunz, C. Huber, Suppression of MHC class I antigens in oncogenic transformants: association with decreased recognition by cytotoxic T lymphocytes, Exp. Hematol. 24 (11) (1996) 1275–1279.
[24] T.H. Inge, S.K. Hoover, B.M. Susskind, S.K. Barrett, H.D. Bear, Inhibition of tumor-specific cytotoxic T-lymphocyte responses by transforming growth factor beta 1, Cancer Res. 52 (6) (1992) 1386–1392.
[25] M.L. Kapsenberg, Dendritic-cell control of pathogen-driven T-cell polarization, Nat. Rev., Immunol. 3 (12) (2003) 984–993.
[26] A. Lanzavecchia, F. Sallusto, Regulation of T cell immunity by dendritic cells, Cell 106 (3) (2001) 263–266.
[27] J. Banchereau, R.M. Steinman, Dendritic cells and the control of immunity, Nature 392 (6673) (1998) 245–252.
[28] J. Banchereau, F. Briere, C. Caux, J. Davoust, S. Lebecque, Y.-J. Liu, B. Pulendran, K. Palucka, Immunobiology of dendritic cells, Annu. Rev. Immunol. 18 (2000) 767–811.
[29] T.B.H. Geijtenbeek, D.S. Kwon, R. Torensma, S.J. Van Vliet, G.C.F. Van Duijnhoven, J. Middel, I.L.M.H.A. Cornelissen, H.S.L.M. Nottet, V.N. KewalRamani, D.R. Littman, C.G. Figdor, Y. Van Kooyk, DC-SIGN, a dendritic cell-specific HIV-1-binding protein that enhances trans-infection of T cells, Cell 100 (5) (2000) 587–597.
[30] Z.-Y. Yang, Y. Huang, L. Ganesh, K. Leung, W.-P. Kong, O. Schwartz, K. Subbarao, G.J. Nabel, pH-dependent entry of severe acute respiratory syndrome coronavirus is mediated by the spike glycoprotien and enhanced by dendritic cell transfer through DC-SIGN, J. Virol. 78 (11) (2004) 5642–5650.
[31] P. Dubruel, B. Christiaens, M. Rosseneu, J. Vandekerckhove, J. Grooten, V. Goossens, E. Schacht, Buffering properties of cationic polymethacrylates are not the only key to successful gene delivery, Biomacromolecules 5 (2) (2004) 379–388.
[32] R.A. Jones, M.H. Poniris, M.R. Wilson, pDMAEMA is internalised by endocytosis but does not physically disrupt endosomes, J. Control. Release 96 (3) (2004) 379–391.
[33] M. Malmsten, G. Siegel, Electrostatic and ion-binding effects on the adsorption of proteoglycans, J. Colloid Interf. Sci. 170 (1) (1995) 120–127.
[34] M. Karlsson, I. Edfors-Lilja, S. Bjornsson, Binding and detection of glycosaminoglycans immobilized on membranes treated with cationic detergents, Anal. Biochem. 286 (1) (2000) 51–58.
[35] L. Thiele, H.P. Merkle, E. Walter, Phagocytosis and phagosomal fate of surface-modified microparticles in dendritic cells and macrophages, Pharm. Res. 20 (2) (2003) 221–228.
[36] L. Thiele, B. Rothen-Rutishauser, S. Jilek, H. Wunderli-Allenspach, H.P. Merkle, E. Walter, Evaluation of particle uptake in human blood monocyte-derived cells in vitro. Does phagocytosis activity of dendritic cells measure up with macrophages? J. Control. Release 76 (1-2) (2001) 59–71.
[37] K.S. Denis-Mize, M. Dupuis, M.L. MacKichan, M. Singh, B. Doe, D. O'Hagan, J.B. Ulmer, J.J. Donnelly, D.M. McDonald, G. Ott, Plasmid DNA adsorbed onto cationic microparticles mediates target gene expression and antigen presentation by dendritic cells, Gene Ther. 7 (24) (2000) 2105–2112.
[38] M. Singh, M. Briones, G. Ott, D. O'Hagan, Cationic microparticles: a potent delivery system for DNA vaccines, Proc. Natl. Acad. Sci. U. S. A. 97 (2) (2000) 811–816.
[39] M. Singh, G. Ott, J. Kazzaz, M. Ugozzoli, M. Briones, J. Donnelly, D.T. O'Hagan, Cationic microparticles are an effective delivery system for immune stimulatory CpG DNA, Pharm. Res. 18 (10) (2001) 1476–1479.
[40] B. Mandal, M. Kempf, H.P. Merkle, E. Walter, Immobilisation of GM-CSF onto particulate vaccine carrier systems, Int. J. Pharm. 269 (1) (2004) 259–265.
[41] F. Takeshita, I. Gursel, K.J. Ishii, K. Suzuki, M. Gursel, D.M. Klinman, Signal transduction pathways mediated by the interaction of CpG DNA with Toll-like receptor 9, Semin. Immunol. 16 (1) (2004) 17–22.
[42] E. Latz, A. Schoenemeyer, A. Visintin, K.A. Fitzgerald, B.G. Monks, C.F. Knetter, E. Lien, N.J. Nilsen, T. Espevik, D.T. Golenbock, TLR9 signals after translocating from the ER to CpG DNA in the lysosome, Nat. Immunol. 5 (2) (2004) 190–198.
[43] J.M. Blander, R. Medzhitov, Regulation of phagosome maturation by signals from toll-like receptors, Science 304 (5673) (2004) 1014–1018.
[44] S.K. Datta, V. Redecke, K.R. Prilliman, K. Takabayashi, M. Corr, T. Tallant, J. DiDonato, R. Dziarski, S. Akira, S.P. Schoenberger, E. Raz, A subset of Toll-like receptor ligands induces cross-presentation by bone marrow-derived dendritic cells, J. Immunol. 170 (8) (2003) 102–110.
[45] A. Heit, T. Maurer, H. Hochrein, S. Bauer, K.M. Huster, D.H. Busch, H. Wagner, Cutting edge: toll-like receptor 9 expression is not required for CpG DNA-aided cross-presentation of DNA-conjugated antigens but essential for cross-priming of CD8 T cells, J. Immunol. 170 (6) (2003) 2802–2805.